N90-28294

A Comparative Study of Infrared Radiance Measurements by an ER-2 Based Radiometer and the Landsat 5 Thematic Mapper (TM-6)

Philip D. Hammer, Francisco P. J. Valero, and Stefan Kinne
NASA Ames Research Center, Moffett Field, CA 94035

1 Introduction

Infrared radiance measurements were acquired from a radiometer on the NASA ER-2 during a coincident Landsat 5 overpass on October 28, 1986 as part of the FIRE Cirrus IFO in the vicinity of Lake Michigan. A comparative study is made to infer microphysical properties of the cirrus cloud field. Radiances are derived from the image by convolving the ER-2 radiometer's effective field of view along the flight path. A multistream radiative transfer model is used to account for the differences in spectral bandwidths, 10.40-12.50 μm for the Landsat band and 9.90-10.87 μm for the radiometer.

2 Instruments

The primary aircraft based instrument employed for this study is a two spectral channel narrow field of view radiometer (NFOV). This instrument was mounted within a pod attached to the fuselage of the NASA ER-2 aircraft. Both channels detect upwelling infrared radiation within a conical field half-angle of 8.3 degrees. The optically sensitive components are electrically calibrated pyroelectric detectors (Valero et al. 1982; Geist and Blevin 1973). A reflective chopper operating at 18 hz alternately exposes the detectors to external radiation and a liquid nitrogen cooled zero-radiation reference. The temperature corrected spectral bandwidths (full width at half maximum) of the interference filters are 6.14-7.14 and 9.90-10.87 μm. In this study only the 10 μm channel bandwidth overlapped one of the Landsat 5 bands: TM-6.

The basic operation principles of the Landsat thematic mapper are described elsewhere (Engel and Weinstein 1983). Standard relations were used for converting the digital pixel counts to radiance and brightness temperature (Markham and Barker 1986). The Landsat 5 TM6 band has an equivalent rectangular spectral bandpass of 10.40-12.50 μm (Wielicki and Parker 1987). Radiances derived from the Planck function integrated over this bandpass agree very well with the Markham and Barker formulas for which this integral is approximated by a simple analytic expression.

3 Analysis

In order to make meaningful comparisons between our NFOV ER-2 radiometer and Landsat image data, a systematic procedure was used to prepare both data sets. First, a geometrically registered satellite image was obtained. Next, the aircraft flight tracks derived from navigational data were adjusted for cloud level winds. Radiances were determined from the image by convolving the ER-2 radiometer's effective field of view with image pixel values along the flight track. The previous two steps require an estimate of the altitude of the optically dominant cirrus layer; this was aided by lidar data. The resulting signals were expressed in spectral bandpass independent units of brightness temperature verses aircraft coordinates. Finally the two sets of radiance measurements were prepared for a 2 channel radiance correlation plot for comparison to model calculations.

4 Model

A discrete ordinates radiative transfer code designed for multi-layered plane-parallel media (Stamnes et al., 1988) was used to calculate radiance values at the corresponding altitudes of the measurements, 19.1 km for the ER-2 and >70 km for Landsat. The number of computational polar angles (streams) was set to 8, as larger values did not generally yield significant differences in the results. 17 atmospheric layers were chosen so as to achieve reasonable homogeneity in temperature (less than 10°K variation) and particle composition within each layer. The upwelling radiance was evaluated at a polar angle of 0 degrees to correspond to the conditions of the measurements.

The assumed ice particle size distributions are described in terms of Mie spheres of a single equivalent radius. Mie calculations were done for a selection of water and ice sphere radii using experimentally determined values for the complex index of refraction of ice (Warren, 1984) and water (Downing and Williams, 1975). Particle concentrations were chosen to yield the desired zero zenith angle optical depths for extinction through all the cloud layers at a reference wavelength of 11.4 μm.

The atmospheric profile input to the model was derived from the 1500 GMT Greenbay radiosonde. Since direct measurements of the Lake Michigan surface temperature were not available the Greenbay surface temperature was used: T_s = 281.9°K. The lake surface was assumed to be Lambertian with a wavelength independent albedo of 0.04. ER-2 based lidar measurements (Spinhirne et al. 1988) indicate that there are two distinct cloud layers over most of the Landsat image extract, with altitude ranges of about 7 to 8 km and 9 to 11 km.

5 Results and Conclusions

Fig. 1a is the Landsat image extract. Fig. 1b shows the ER-2 radiometer and Landsat signals along the flight track in units of brightness temperature. Figs. 2 and 3 are correlation plots. The ER-2 and satellite scales are expressed in radiance units ($Wm^{-2}sr^{-1}$) for the instruments' respective bandpasses. The measured data points of Fig. 2 (represented as small dots in Fig. 3) are derived from the data represented in Fig. 1b. Data is distinguished as to ice or water according to the lidar plot of Fig. 1c.

The model calculations are plotted as connected sets of specific symbol types. Each set corresponds to radiance results for a range of optical depths using particles with particular radius selections. Beginning at the upper right convergence point the optical depth values (referenced at 11.4 μm) are 0, 0.125, 0.25, 0.375, 0.5, 0.625, 0.75, 1.0, 1.25, 1.5, and 2.0. For the standard model (connected unfilled symbols in Fig. 2 and solid symbols in Fig. 3) a two layer cloud profile was chosen with ice spheres in the upper layer having about half the effective radius of spheres in the lower layer. The 11.4 μm optical depths of the lower and upper layers were set equal. Unfilled symbols in Fig. 3 represent a profile with water drops present in the lower layer and nothing in the upper. The following conclusions are based on comparisons of measured radiances with model results on the correlation plots:

1. Assuming the above standard model, ice particles with equivalent sphere radii of 8 to 15 μm for the upper layer and 15 to 30 μm for the lower layer may be inferred. This contrasts with particle sizes typically greater than 100 μm determined by in-situ measurements. The lack of sensitivity of the in-situ probes to small ice crystals and the uncertainties in ice-water content determinations causes difficulties in resolving whether a large number of small particles are actually present as opposed to complex large particles with small protrusions. The combined cloud extinction optical depth for both layers at the reference wavelength of 11.4 μm ranges from about 0.3 to 2.

2. Assuming a 1-layer lower water cloud yields results consistent with approximately 8 μm radii water droplets. This compares with in-situ measurements of radii about 4 μm. Distinguishing measurements made with water clouds present from those made for just ice clouds gives no apparent

separation on the correlation plots. Thus water and ice clouds cannot be distinguished from the correlation plots alone under the conditions of this case study. The optical depth scale is only moderately changed (< 20%) from the 2-layer ice model results.

3. Limits on the estimated instrument error may be established by means of self-consistency of the model results. Specifically, if Landsat radiances values were too high, the inferred water cloud droplet sizes would be unrealistically large. Thus our retrieval of relatively small ice crystals cannot be attributed to a Landsat (nor an ER-2 radiometer) calibration error.

References

[1] Downing, H. D. and D. Williams, 1975: Optical constants of water in the infrared. *J. Geophys. Res.*, **80**, 1656-1661.

[2] Engel, J. L. and O. Weinstein, 1983: The Thematic Mapper - An Overview. *IEEE Trans. Geosci. Remote Sensing,* Vol. GE-21, No. 3: 258-265.

[3] Geist, J. and W. R. Blevin, 1973: Chopper-stabilized null radiometer based upon an electrically calibrated pyroelectric detector. *Appl. Opt.*, **12**, 2532-2535.

[4] Markham, B. L., and J. L. Barker, 1986: Landsat MSS and TM post-calibration dynamic ranges, exoatmospheric reflectances and at-satellite temperatures. *EOSAT Landsat Technical Notes,* August 1986, 3-8.

[5] Spinhirne, J. D., D. L. Hlavka, W. D. Hart, 1988: ER-2 lidar observations from the October 1986 FIRE cirrus experiment. *NASA Technical Memorandum 100704*, NASA Goddard Space Flight Center, June 1988, 49pp.

[6] Stamnes, K., S. C. Tsay, W. J. Wiscombe and K. Jayaweera, 1988: A general-purpose numerically stable computer code for discrete-ordinate-method radiative transfer in scattering and emitting layered media. *International Radiation Symposium Abstracts, Lille, France*, August 18-24, p. 186.

[7] Valero, F. P. J., W. J. Y. Gore, and L. P. M. Giver, 1982: Radiative flux measurements in the troposphere. *Appl. Opt.*, **21**, 831-838.

[8] Warren, S. G., 1984: Optical constants of ice from the ultraviolet to the microwave. *Appl. Opt.*, **23**, 1206-1225.

[9] Wielicki, B. A. and L. Parker, 1987: Intercalibration of landsat thematic mapper (TM) and ER-2 MAMS during the FIRE cirrus IFO-I October 28, 1986. *NASA Langley Technical Report*

[10] Wielicki, B. A., J. T. Suttles, A. J. Heymsfield, R. M. Welch, J. D. Spinhirne, L. Parker, and R. F. Arduini, 1988: FIRE cirrus on 10/28/86: Landsat; ER-2; King air; theory. FIRE Science Team Workshop, Vail CO, July 1988.

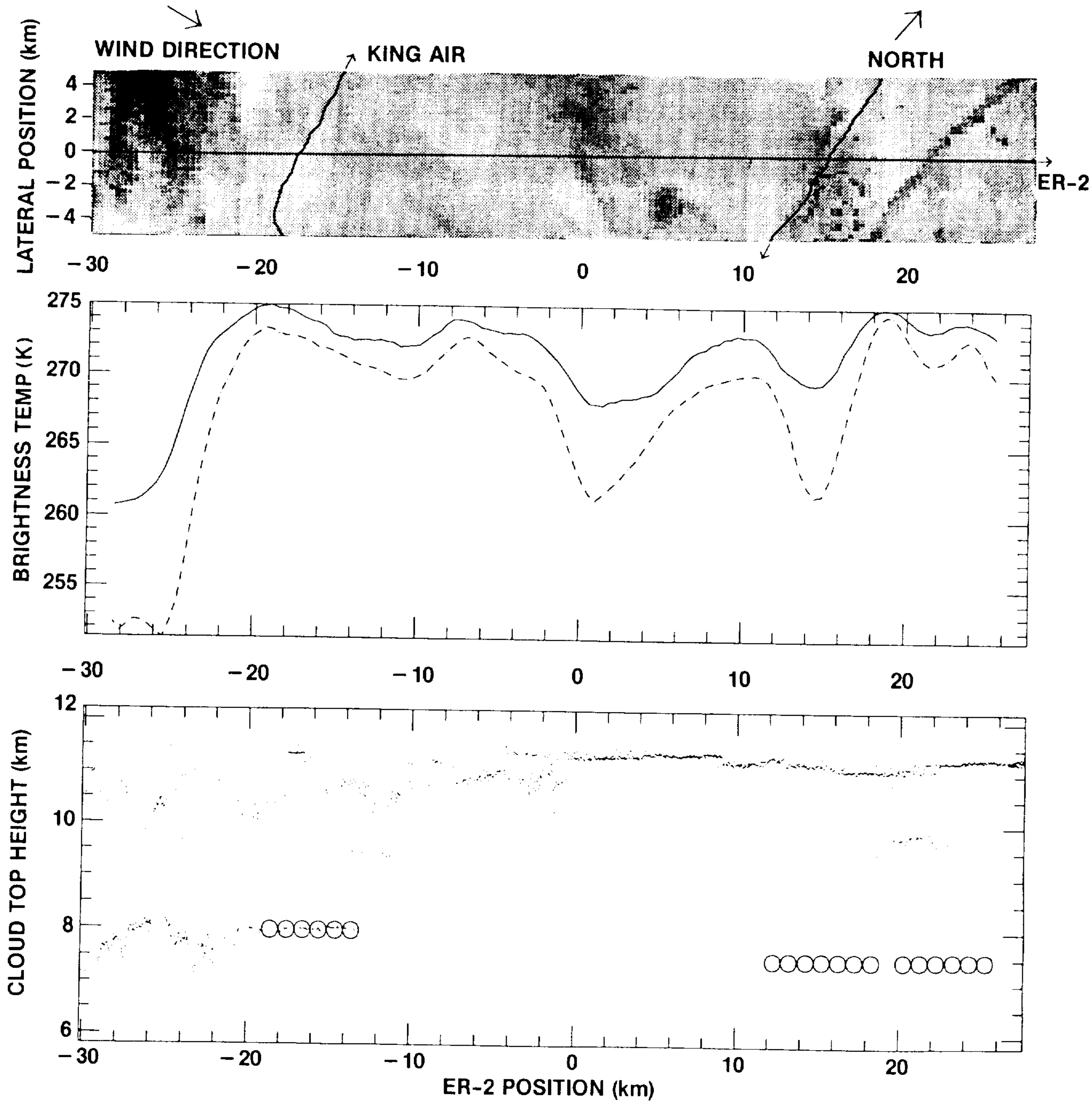

WIND DIRECTION
KING AIR
NORTH
ER-2
LATERAL POSITION (km)
4
2
0
−2
−4
−30
−20
−10
0
10
20
BRIGHTNESS TEMP (K)
275
270
265
260
255
CLOUD TOP HEIGHT (km)
12
10
8
6
ER-2 POSITION (km)

FIG 2

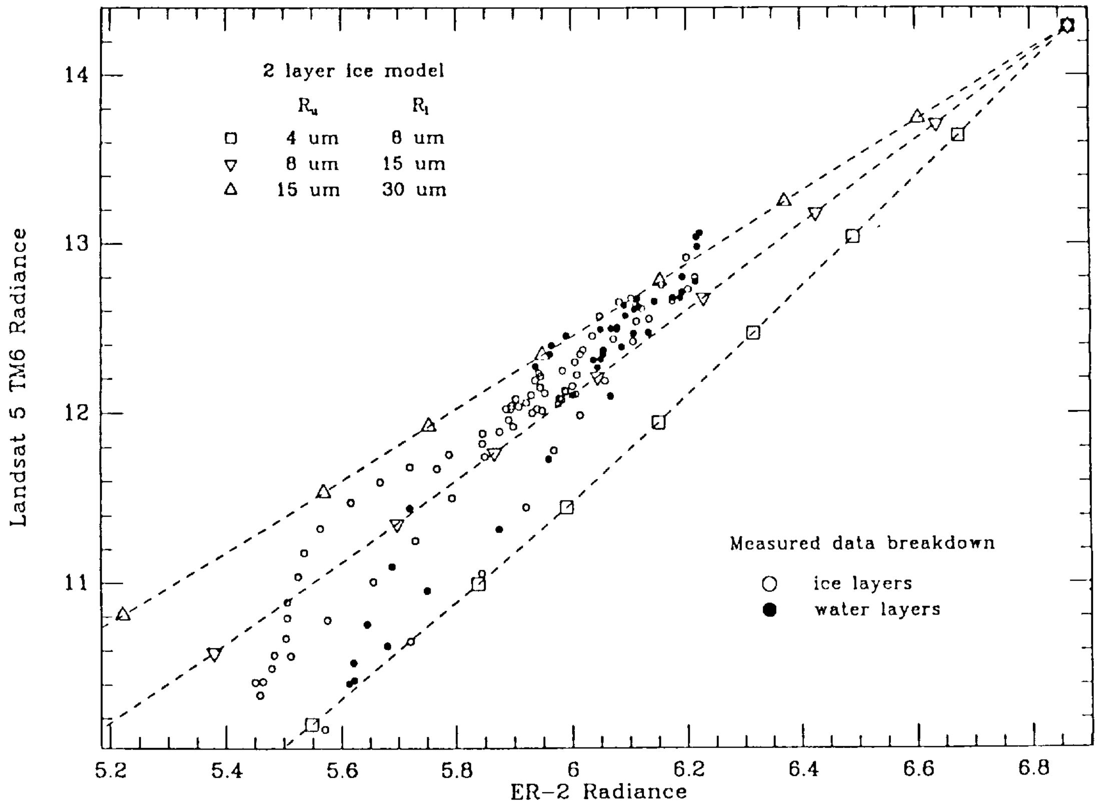

NASA-Ames

7-JUL-1989 16:10:39

FIG 3